DOI: 10.21062/mft.2021.037 http://www.journalmt.com

Modeling of A New Coupler Critical Dimensions (CCD) for Mobility Analysis

Md Hazrat Ali[1] (ORCID: 0000-0003-0428-957X), Nazim Mir-Nasiri[2] (ORCID: 0000-0002-4143-3502), Manafaddin Namazov[2] (ORCID: 0000-0003-1119-2442), Husseyn Mirzayev[2] (ORCID: 0000-0002-1977-3914), M. Hassan Tanveer[3] (ORCID: 0000-0001-9266-6368)
[1]Mechanical and Aerospace Engineering Department, Nazarbayev University in Nus-Sultan. Kabanbay batyr 53, 010000 Nur-Sultan. Kazakhstan, E-mail: md.ali@nu.edu.kz; mtanveer@kennesaw.edu
[2]Engineering Faculty,Baku Engineering University, Azerbaijan.
[3]Department of Robotics and Mechatronics Engineering, Kennesaw State University, Marietta, GA, USA

A new Coupler Critical Dimensions (CCD) approach to define mobility criteria (crank, rocker conditions, or existence) for linkage mechanisms has been presented in this paper. The concept is critical to design and analyze the extreme lengths of a mechanism coupler link when the mechanism is at the extreme of its existence or changing its mobility condition. The method leads a set of expressions of the constant mechanism parameters that can define the mechanism's coupler link's exact dimensional limits. These expressions present sufficient and necessary dimensional conditions for the mechanism's existence and become a turning point to change mobility from a crank to a rocker and vice versa. The mechanism reaches its change-point configuration at the boundaries of the coupler dimensions. The mechanism may switch from one work function to another or from existence to non-existence. The method has been successfully applied to the planar 4R, spatial RSSR, and planar multiloop linkage mechanisms. The obtained results prove the effectiveness and accuracy of the method in defining the limits of the mechanism rotatability conditions or existence in general. The crank condition is essential to couple it with the motor or engine. If the mechanism input link is not a crank (i.e., it has a possibility of full rotation), the motor may crash the entire mechanism. Rotatabilty of the input link is a fundamental concept in machines and mechanisms.

Keywords: Additive Manufacturing, 3D Printing, Composite Materials, Material Properties

1 Introduction

Mobility analysis of four-bar linkages is a well-established field. For many years, the Grashof criterion has been applied to predict planar four-bar linkage mechanisms' mobility. Chang et al. [1] justified Grashof's theorem in terms of the occurrence of stationary configurations and uncertainty configurations of four-link chains. They examined the link length relations at stationary configurations and uncertainty configurations based on the triangle inequality. Five-bar Grashof's criteria were transformed into an extended version, namely law for N-bar kinematic chains, by Ting et al. [2]. They provided proof of the theorems concerning the mobility of planar N-bar linkages based on the assemblability condition of N-bar linkages and the angle's revolvability condition. Ting and Wang [3] presented a detailed analysis for the full rotatability of 6-bar and geared 5-bar linkages, irrespective of the selection from the reference links or input joints. They have presented a generic method to detect the dead center positions and the relevant branches. Gogate [4] presented a rotatability analysis of Watt 6-link mechanisms using an evolutionary optimization algorithm. Midha et al. [5] have used the triangle inequality concept in formulating the mobility conditions for a planar 4-bar linkage. More significantly, a manifest graphical interpretation was offered, enabling an expeditious mobility determination. Angeles et al. [6] have reduced the mobility analysis of 4-bar linkages to find the global extrema from a quadratic function of a cylinder, leading to the geometric problem of finding the intersections of a circle and a hyperbola. Li et al. [7] have investigated planar parallel mechanisms' rotatability by highlighting the crank conditions concerning link parameters. Their research has led to the classification of three types of crank existing conditions, including 3-crank's, 6-crank's, and 9-crank's of 3-RRR planar parallel mechanisms. Bai [8], [9] has recently revisited planar four-bar linkages' mobility problem. The mobility has analyzed the range of rotation of the coupler link for a special case of its full rotatability when the coupler link drives the linkage. They have formulated a new concept of couple curve rotation by the constraint triangle. The mobility is analyzed in terms of the coupler angle range by a geometric approach.

Many attempts have been made to derive direct rotatability criteria for the RSSR and other types of spatial linkages. Most of them, such as Bottema [10], Cheng et al. [11], Nolle et al. [12], Pamidi et al.[13], Ting et al.[14] are mainly based on the analysis of discriminant function, and some used geometrical concepts [15]. However, compared to the Grashof criterion, the resulting mobility criteria appeared to be quite complicated and are based on lengthy mathematical treatment. Gupter et al. [16] attempted to derive a direct rotatability criterion for spherical four-bar linkages. They have achieved a solution to some values of constant twist angles. However, the solutions do not provide sufficient conditions for the mechanism to exist and work either as a crank-rocker, a drag-link (double crank), or a double-rocker mechanism. Kazerounian and Solecki [17] have introduced equation $Z = (\cos 2\mu) - 1 = 0$, where μ is the transmission angle of an R-S-S-R four-bar linkage. They have defined the linkage's mobility by the number of real roots of this equation. Furthermore, it is believed that there were no serious attempts to solve a similar problem for the multiloop linkage mechanisms. Another work aimed to design support and a tension mechanism for a wheel-tracked chassis of a mine-clearing machine [18]. In separate research, dynamic analysis of the crank mechanism is designed, and a connecting rod is modelled with three different manners. In the first case, the connecting rod is modelled as a rigid body; in the second case, it is modelled with two mass points, and in the third case, the rod is modelled with three mass points [19].

The method of critical coupler dimensions introduced in this work yields much more straightforward and readable closed-form expressions for the crank criteria used for the bimodal or multiloop mechanisms. The method is based on deriving an explicit expression of coupler link length as a function of all other constant and variable parameters of a linkage mechanism using any appropriate kinematic analysis method. Theoretically, the mechanism existence (possibility to assemble) and possible mobility can be defined in between the limits (maximum and minimum critical values) of the coupler lengths identified for all possible values of mechanism variable parameters. Therefore, the coupler explicit expression becomes a multivariable function of all variables and the mechanism's constant parameters. By defining stationary points, i.e., points where partial derivatives of the function with respect to variable parameters become zero, it is possible to calculate maxima and minima of the coupler function, namely coupler lengths. These points will define the mechanism existence or changepoint configurations' extremes when linkage switches from one type of mobility to another (for example, from double-crank to crank-rocker. The following analysis of various linkage mechanisms proves the proposed theory's validity.

2 Materials and Methods

2.1 Mobility Analysis of Four-bar Planar Linkage Mechanism

Figure 1 shows a four-bar planar linkage mechanism, where OC is predefined as a ground link. In Fig. 1, i, j, e1, e2, and e3 are the unit vectors associated with the axes of the reference frame and mechanism links, respectively; φ1, φ2, φ3 are the angles that links 1, 2, and 3 make with X-axis of the frame. Using a vector method, one can easily derive the multivariable target function for the couple-link AB length (dotted line).

$$AB^2 = OA^2 + BC^2 + OC^2 + 2\cdot OC\cdot BC\cdot\cos(\varphi_3) - 2\cdot OC\cdot OA\cdot\cos(\varphi_1) - \\ - 2\cdot BC\cdot OA\cdot\cos(\varphi_1)\cdot\cos(\varphi_3) - 2\cdot BC\cdot OA\cdot\sin(\varphi_1)\cdot\sin(\varphi_3) \quad (1)$$

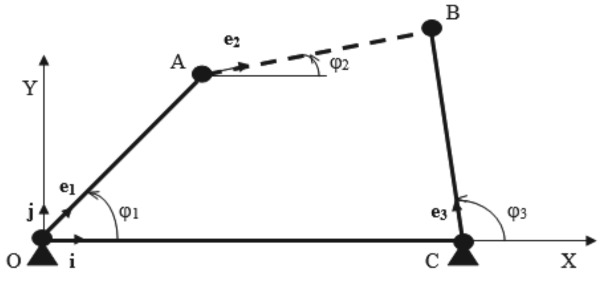

Fig. 1 *Schematic diagram of the four-bar planar linkage mechanism.*

From Eq. (1), it is obvious that AB is a function of lengths of constant parameters BC, OC, OA, and two variable angles φ1, φ3. Following the proposed method, the partial derivatives of Eq. (1) with respect to variables φ1, φ3 can be derived and equated to zero. Subsequent analysis shows that Eq. (1) reaches its stationary points if the following is satisfied:

$$\sin(\varphi_3) = \sin(\varphi_1) = 0 \quad (2)$$

This will define the four-bar linkage's change point configuration when OA aligns with BC. Equation (2) holds true for combinations of angles, such as a) φ1= 0°, φ3 = 0°; b) φ1= 180°, φ3 = 0°; or c) φ1= 0°, φ3 = 180°; and d) φ1= 180°, φ3 =180°. Substituting them into (1), we can get analytical expressions for the four possible critical dimensions of coupler link AB. They are as follows:

$$AB_a^2 = (OC + BC - OA)^2 \quad (3)$$

$$AB_b^2 = (OA + BC + OC)^2 \quad (4)$$

$$B_c^2 = (BC + OA - OC)^2 \quad (5)$$

$$AB_d^2 = (OC + OA - BC)^2 \quad (6)$$

The coupler critical dimension ABb2 in Eq. (4) is the largest among Eqs. (3), (4), (5), and (6). This dimension of coupler ABb2 in Eq. (14) corresponds to the machine's configuration when it has reached the verge of its existence and will not be considered for possible crank mobility conditions. The remaining expressions in Eqs. (3), (5) and (6) are sufficient to derive crank criteria for the four-bar planar linkage mechanism. The requirements are obtained by comparing the lengths of AB from Eqs. (3) (5) and (6) with each other for all possible pair combinations (six possible combinations) and testing the crank condition numerically with a computer. The obtained criteria are as follows:

i) Double-crank mechanism occurs when link OC is the smallest one (OC<OA, OC<BC) and AB is within the range

$$OC + /OA - BC/ \leq AB \leq OA + BC - OC \quad (7)$$

ii) Crank-rocker mechanism occurs when link OA is the smallest one (OA<OC, OA<BC) and AB is within the range

$$OA + /OC - BC/ \leq AB \leq OC + BC - OA \quad (8)$$

iii) Double-rocker mechanism occurs when conditions (i) and (ii) do not satisfy and AB is within the range smallest

$$(AB_1, AB_3, AB_4) \leq AB \leq OA + OC + BC \quad (9)$$

The equal sign in Eq. (7) to (9) means the linkage has reached its change-point configuration. In this configuration, coupler AB's dimension corresponds to its boundary value when it changes its work function from one to another in Eqs. (7), (8), or has reached the verge of its existence in Eq. (9). The obtained results are consistent with the Grashof criteria of rotatability. However, criteria in Eqs. (7) to (9) are more suitable and takes less computation to synthesize four-bar linkages than Grashof criteria because it requires only one inequality expression instead of several conditions defined by the Grashof method.

2.2 Mobility Analysis of Four-Bar Spatial Linkage Mechanism

The results are compared to available experimental wind tunnel data to ensure the calculations' validity and accuracy. Normal force coefficient and base drag coefficient are compared as a function of Mach number and angle of attack. Two typical projectile configurations (as shown in Figs. 2 and 3) are selected for this purpose. The specifications of the models and test conditions are explained below.

The schematic diagram of the RSSR linkage mechanism is shown in Fig. 2. In Fig. 2, i, j, k, e1, e2, e3, e4, and e5 are the unit vectors associated with the coordinate axes and mechanism links, respectively. For simplicity, link OC (vector e2) is predefined as a ground link located on the X-Y plane, and axes of the input joint O (vector i) and output joint C (vector e3) are also located on the X-Y plane but not parallel to each other. Fig. 2 shows that (φ2, i + φ3,2) is the angle between input and output joints on the X-Y plane. In this configuration, φ1,j is mechanism variable input angle associated with link OA (measured between j and e1), and φ4,5 is mechanism variable output angle associated with link BC (estimated between e4 and e5). e3 is perpendicular to e4.

The vector method can carry the kinematic analysis of the spatial RSSR linkage mechanism. That analysis eventually leads to the target multivariable function for the length of couple-link AB (dotted line):

$$AB^2 = OA^2 + OC^2 + BC^2 - 2\cdot OC\cdot BC\cdot \sin(\varphi_{3,2})\cdot \cos(\varphi_{4,5}) - 2\cdot OC\cdot OA\cdot \sin(\varphi_{2,i})\cdot \cos(\varphi_{1,j}) - \\ -2\cdot BC\cdot OA\cdot \cos(\varphi_{2,i}+\varphi_{3,2})\cdot \cos(\varphi_{4,5})\cdot \cos(\varphi_{1,j}) - 2\cdot BC\cdot OA\cdot \sin(\varphi_{4,5})\cdot \sin(\varphi_{1,j}) \quad (10)$$

From Eq. (10), it is obvious that AB is a function of lengths of constant parameters OA, BC, OC, and two variable angles φ1,j and φ4,5. Partial derivatives of function in Eq. (10) with respect to variables φ1,j and φ4,5 can be derived and equated to zero. Subsequent analysis shows that function in Eq. (10) reaches its stationary points if the following satisfy

$$\sin(\varphi_{1,j}) = \sin(\varphi_{4,5}) = 0 \quad (11)$$

Equation (11) defines the change point configuration of four-bar RSSR linkage. The condition in Eq. (11) holds true for combinations of two angles, such as a) φ1,j= 0°, φ4,5 = 180°; b) φ1,j= 180°, φ4,5 =0°; or c) φ1,j= 0°, φ4,5 = 0°; and d) φ1= 180°, φ3 =180°. Substituting them into Eq. (1) we can get analytical expressions for the four possible critical dimensions of coupler link AB. They are as follows:

$$AB_a^2 = OA^2+OC^2+BC^2+2\cdot OC\cdot BC\cdot \sin(\varphi_{3,2}) - 2\cdot OC\cdot OA\cdot \sin(\varphi_{2,i}) + 2\cdot BC\cdot OA\cdot \cos(\varphi_{2,i}+\varphi_{3,2}) \quad (12)$$

$$AB_b^2=OA^2+OC^2+BC^2-2\cdot OC\cdot BC\cdot sin(\varphi_{3,2})+2\cdot OC\cdot OA\cdot sin(\varphi_{2,i})+2\cdot BC\cdot OA\cdot cos(\varphi_{2,i}+\varphi_{3,2}) \quad (13)$$

$$AB_c^2=OA^2+OC^2+BC^2-2\cdot OC\cdot BC\cdot sin(\varphi_{3,2})-2\cdot OC\cdot OA\cdot sin(\varphi_{2,i})-2\cdot BC\cdot OA\cdot cos(\varphi_{2,i}+\varphi_{3,2}) \quad (14)$$

$$AB_d^2=OA^2+OC^2+BC^2+2\cdot OC\cdot BC\cdot sin(\varphi_{3,2})+2\cdot OC\cdot OA\cdot sin(\varphi_{2,i})-\cdot BC\cdot OA\cdot cos(\varphi_{2,i}+\varphi_{3,2}) \quad (15)$$

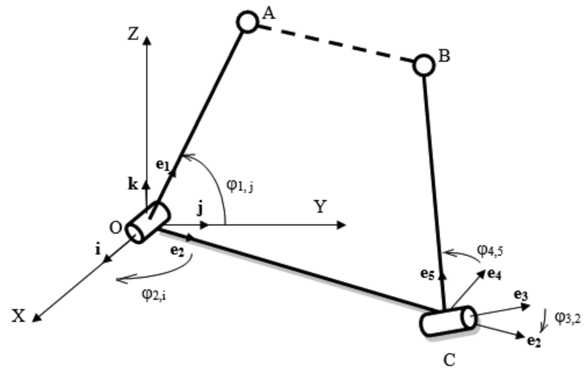

Fig. 2 *Schematic diagram of the RSSR spatial linkage mechanism.*

It can be seen that ABc2 in Eq. (14) is the smallest among all the critical dimensions defined by Eqs. (12), (13), (14), and (15). This dimension of coupler ABc2 (14) corresponds to the configuration of the mechanism when it has reached the extreme of its existence and will not be considered for a possible crank mobility condition. The expressions in Eqs. (12), (13) and (15) are sufficient to derive crank criteria for the RSSR spatial linkage mechanism. The criteria are derived by comparing the critical lengths of AB from Eqs. (12), (13), and (15) with each other for all possible pair combinations (six possible combinations) and testing the crank condition numerically with a computer. The obtained criteria are as follows:

i) *double-crank mechanism occurs when link $OC\cdot sin(\varphi 2,i) < BC\cdot cos(\varphi 2,i+\varphi 3,2)$;*
$OC\cdot sin(\varphi 3,2) < OA\cdot cos(\varphi 2,i+\varphi 3,2)$ and AB is within the range

$$AB_d^2\,(15) \leq AB^2 \leq AB_a^2\,(12) \quad (\text{if } BC\cdot sin(\varphi_{3,2}) < OA\cdot sin(\varphi_{2,i}) \quad (16)$$

$$AB_d^2\,(15) \leq AB^2 \leq AB_b^2\,(13) \quad (\text{if } BC\cdot sin(\varphi_{3,2}) > OA\cdot sin(\varphi_{2,i})) \quad (17)$$

ii) *crank-rocker mechanism occurs when link $OA\cdot sin(\varphi 2,i) < BC\cdot sin(\varphi 3,2)$;*
$OA\cdot cos(\varphi 2,i+\varphi 3,2) < OC\cdot sin(\varphi 2,i)$ and AB is within the range

$$AB_b^2\,(13) \leq AB^2 \leq AB_a^2\,(12) \quad (\text{if } BC\cdot cos(\varphi_{2,i}+\varphi_{3,2}) < OC\cdot sin(\varphi_{2,i})) \quad (18)$$

$$AB_b^2\,(13) \leq AB^2 \leq AB_d^2\,(15) \quad (\text{if } BC\cdot cos(\varphi_{2,i}+\varphi_{3,2}) > OC\cdot sin(\varphi_{2,i})) \quad (19)$$

iii) *double-rocker mechanism occurs when conditions (i) and (ii) do not satisfy, and AB is within the range*

$$AB_c^2\,(14) \leq AB^2 \leq \text{largest } [AB_a^2\,(12), AB_b^2(13), AB_d^2(15)] \quad (20)$$

The equal sign in Eqs. (16) to (20) means the linkage has reached its change-point configuration. In this configuration, coupler AB's dimension corresponds to its boundary value when the mechanism switches its work functions n Eqs. (16), (17), (18), (19), or has reached the verge of its existence in Eq. (20).

2.3 Mobility Analysis of Multi-loop Planar Linkage Mechanism

For simplicity of analysis, all three fixed pivots F, O, and C are taken on a single horizontal ground line. In Fig. 3, i, j, e1, e2, e3, e4, e5, e6 are the unit vectors associated with the axes of the reference frame and mechanism links, respectively; φ1, φ2, φ3, φ4, φ5, and φ6 are the angles that links 1, 2, 3, 4, 5, and 6 make with X-axis of the frame. Angle α is a constant angle that permanently exists between e2 and e4. That means there exists the following expression between φ4 and φ2 angles:

$$\varphi_4 = \varphi_2 + \alpha \quad (21)$$

Figure 3 shows a Stephenson type six-bar planar linkage mechanism below.

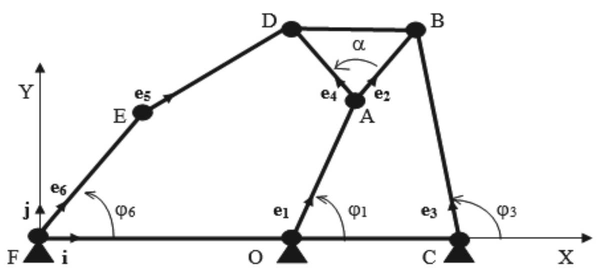

Fig. 3 *Schematic diagram of the six-bar planar linkage mechanism.*

By taking link OA as an input link, the kinematic analysis of the linkage mechanism (Fig. 3) can be carried out by vector method based on the following two loops equations:

$$OA \cdot e_1 + AB \cdot e_2 = OC \cdot i + BC \cdot e_3 \qquad (22)$$

$$FO \cdot i + OA \cdot e_1 + AD \cdot e_4 = FE \cdot e_6 + ED \cdot e_5 \qquad (23)$$

In a multiloop mechanism (Fig. 3), Eqs. (22) and (23) are connected via expression in Eq. (21). The mechanism in Fig. 3 can be viewed as an extension of the mechanism shown in Fig. 1 by adding a loop OADEF to it. The link OA remains an input link for both loops of the multiloop mechanism in Fig. 3. Therefore, the mobility conditions derived in Section 2 remain valid for the loop OABC in Fig. 3 as well. The change point configuration in the loop OABC occurs when sin (φ1) = 0, i.e. i = e1 in Eq. (2). At that configuration, the multiloop mechanism takes the position, as shown in Fig. 4, and acts as a four-bar linkage with regard to loop FEDAO.

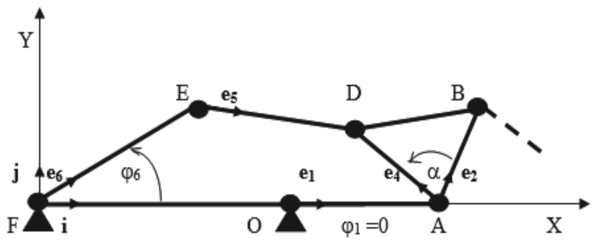

Fig. 4 *Multiloop mechanism.*

The mobility condition of four-bar linkage in Eq. (7) can then be applied separately to the loop FEDAO (with coupler ED) to achieve full rotatability of links FE and AD regardless of rotatability conditions in the loop OABC. Full rotatability of links FE and AD can be achieved when FA=FO+OA is the smallest one (FA<FE, FA<AD) and ED are within the range:

$$FA + /FE - AD/ \leq ED \leq FE + AD - FA \qquad (24)$$

The condition (24) does not depend on a constant angle α. Equations (7), (8), (9), and (24) establish simultaneous change point configurations for both loops OABC and FEDAO. In connection to the entire multiloop planar mechanism, the following statements are true:

i) *triple-crank (OA, FE, BC) mechanism* occurs when Eqs. (7) and (24) are satisfied
ii) *double-crank (OA, FE) - rockers (BC)* occurs when Eqs. 8) and (24) are satisfied
iii) *triple-rocker (OA, FE, BC) mechanism* occurs when Eqs. (9) and (24) are satisfied
iv) the *mechanism does not exist* if none of the above conditions are satisfied.

3 Performance evaluation

Most of the past works on the rotatability criteria (mentioned in the introduction) are mainly based on discriminant function analysis, and some used geometrical concepts. However, the resulting mobility criteria appeared to be quite complicated and are based on lengthy mathematical modeling. As an example, Gupter et al. [16] attempted to derive a direct rotatability criterion for spherical four-bar linkages. They have achieved a solution to some values of constant twist angles. However, the solutions do not provide sufficient conditions for the mechanism to exist and work either as a crank-rocker, a drag-link (double crank), or a double-rocker mechanism. The results achieved in this research demonstrate a unique method (coupler critical dimensions) that can easily be applied to any single or multiloop mechanism (planar and spatial) to determine all possible work functions and defines precisely change point configurations. For example, results achieved for the multiloop planar mechanism (Fig. 4), i.e., equation (24), are unique and not defined by any other researcher in this field. Similarly, results achieved for RSSR spatial mechanism (Fig. 2), i.e., work functions equations (16 – 20), were not discovered by the existing works. That means the presented research outcome (CCD) has a significant contribution to the field of mobility analysis of linkage mechanisms and has the potential to be applied to other types of spatial and multiloop planar linkage mechanisms.

4 Conclusion

The present paper introduces a new method of critical coupler dimensions to analyze the mobility or crank condition for single-loop planar and spatial linkage mechanisms and a multiloop planar mechanism. This method's advantage is that it can be easily applied to any linkage mechanism; it does not require a complete kinematic analysis of the mechanism and analyzes its discriminant function. Typically, researchers usually did it. The method that works on the input-output function of the mechanism leads directly to the coupler links critical (boundary) dimensions when the mechanism abruptly switches its mobility function, for example, from double-crank to crank-rocker and vice versa. It also shows the limiting values for the coupler link in connections to other links when the mechanism ceases to exist. This research's vital contribution to the mobility of linkages is that the first time introduces a complete set of relationships between constant parameters of planar and spatial four-bar mechanisms that cause them to operate either as a double-crank or crank-rocker or double-rocker one. It also introduces a complete set of relationships between constant parameters of a multiloop planar mechanism that causes it to work either as a triple-crank or double-crank-rocker, or triple-rocker mechanism.

References

[1] CHANG, W. T., LIN, C. C., & WU, L. I. (2005). A Note on Grashof's Theorem. Journal of Marine Science and Technology,13(4), pp. 239-248.

[2] TING, K., & LIU, Y. (1991). Rotatability Laws for N-Bar Kinematic Chains and Their Proof. Journal of Mechanical Design,113(1), pp. 32-39.

[3] TING, K., WANG, H., CUE, C., & CURRIE, K., R. (2010). Full Rotatability and Singularity of Six-Bar and Geared Five-Bar Linkages. *Journal of Mechanisms and Robotics,* 2(1), pp. 100-1-9.

[4] GOGATE, G. R. (2018). Explicit input link rotatability analysis of Watt six-link mechanisms. *Journal of Mechanical Science and Technology*,32(7), pp. 3407-3417.

[5] MIDHA, A., ZHAO, Z., & HER, I. (1985). Mobility Conditions for Planar Linkages Using Triangle Inequality and Graphical Interpretation. *Transmissions and Automation in Design*,107(3), pp. 1-6.

[6] ANGELES, J., & BERNIER, A. (1987). A General Method of Four-Bar Linkage Mobility Analysis. *Journal of Mechanisms, Transmission, and Automation in Design*,109(2), pp. 197-203.

[7] LI, R., & DAI, J. S. (2009). Crank conditions and rotatability of 3-RRR planar parallel mechanisms. *Science in China Series E: Technological Sciences*, 52, pp. 17-48.

[8] BAI, S. (2017). Geometric analysis of coupler-link mobility and circuits for planar four-bar linkages. *Mechanism and Machine Theory*,118, pp. 53-64.

[9] BAI, S. (2017). Coupler-Link Mobility Analysis of Planar Four-Bar Linkages. *New Trends in Mechanism and Machine Science*, Springer, pp. 41-49.

[10] BOTTEMA, O. (1971). The Motion of the Screw Four-Bar, *Journal of Mechanisms*, Vol. 6, 1971, pp 69-79.

[11] CHENG, J. C., KOHLI, D. (1992). Synthesis of Mechanisms Including Circuit Defects and Input-Crank Rotatability, *Proceedings Mechanical Design and Synthesis, ASME*, USA, 1992, pp 111-119.

[12] NOLLE, H. (1969). Ranges of Motion Transfer by the R-G-G-R Mechanisms, *Journal of Mechanisms*, Vol. 4, 1969, pp 145-157.

[13] PAMIDI, P.R., FREUDENSTEIN, F. (1975). On the Motion of a Class of Five-link, R-C-R-C-R, Spatial Mechanisms, *Journal of Engineering for Industry*, Feb. 1975, pp 334-339.

[14] TING, K., XIAOHONG, D. (1994). Branch, Mobility Criteria, and Classification of RSSR and Other Bimodal Linkages, *Proceedings Mechanism Synthesis and Analysis, ASME*, USA, 1994, pp 303-310.

[15] LUO, H. T. (1992). Bidirectional Extreme Convergency Method (BECM) to Identify the Mobility Regions of the RSSR Mechanism, *Proceedings 22nd Biennial Mechanisms Conference, ASME*, USA, Vol.47, 1992, pp 151-159.

[16] GUPTA, K. C., MA, R. (1995). Direct Rotatability Criterion for Spherical Four-bar Linkages, *Journal of Mechanical Design*, Dec., Vol. 117, 1995, pp 597-600.

[17] KAZEROUNIAN, K., & SOLECKI, R. (1993). Mobility analysis of general bi-modal four-bar linkages based on their transmission angle. *Mechanism and Machine Theory*,28(3), 437-445.

[18] BLATNICKÝ M, DIŽO J, HARUŠINEC J. (2020). Modification of a design of a wheel-tracked chassis of a mine-clearing machine. *Manufacturing Technology*. 2020; 20(3), pp. 286-292. doi: 10.21062/mft.2020.044.

[19] MINÁRIK M, BODNÁR F. (2019). Dynamic Analysis of the Crank Mechanism through the Numerical Solution. *Manufacturing Technology*. 2019; 19(6), pp. 1003-1009. doi: 10.21062/ujep/410.2019/a/1213-2489/MT/19/6/1003.